Engineering Failure Analysis 105 (2019) 215–226

Contents lists available at ScienceDirect

Engineering Failure Analysis

journal homepage: www.elsevier.com/locate/engfailanal

Effect of oxygen partial pressure on oxidation behavior of ferritic stainless steel AISI 441 at high temperatures

Maria de Fátima Salgado[a,b,*], Iure S. Carvalho[a], Rafael S. Santos[a], João Alberto Santos Porto[a,b], O.V. Correa[c], L.V. Ramanathan[c], Ayrton de Sá Brandim[b], Vanessa F.C. Lins[d]

[a] Universidade Estadual do Maranhão – CESC/UEMA, Brazil
[b] Programa de Pós-Graduação Engenharia de Materiais, – PPGEM – IFPI, Brazil
[c] Instituto de Pesquisa Energeticas E Nucleares – IPEN, Brazil
[d] Universidade Federal de Minas Gerais, Brazil

ARTICLE INFO

Keywords:
AISI 441
Stainless steel
Synthetic air
Oxidation
Argon

ABSTRACT

In this investigation the oxidation behavior of AISI 441 stainless steel (SS) in the range from 850 °C to 950 °C was determined during 50 h in two different atmospheres: (a) synthetic air in a tubular oven; (b) argon with 1 ppm of O_2 in a thermal balance. The oxidation kinetics was determined from the measured mass change as a function of oxidation time. Examination of the microstructure of the oxides and determination of their chemical composition were performed by using scanning electron microscopy (SEM), energy dispersive X-ray spectroscopy (EDS) and glancing angle X-ray diffraction (GAXRD). Chemical analyses showed that films formed on the AISI 441 steel surface consisted mostly of chromium oxide but manganese, iron, titanium and silicon oxides were found in the oxidized layer. In synthetic air, the steel oxidation rate increased gradually as the temperature increased, but in the argon atmosphere with 1 ppm of oxygen, the highest oxidation rate was observed at 900 °C and the lowest at 950 °C.

1. Introduction

Many studies have reported the oxidation behavior of AISI 441 ferritic stainless steel. However, published data about oxide layer growth on AISI 441 at high temperatures is scarce. Salgado et al. [1] studied the cyclic oxidation resistance of AISI 439 and AISI 441 ferritic stainless steels (FSS) at a temperature typically encountered in a muffler (300 °C). High purity inert gases are commonly used as protective atmospheres in heat treatment or thermo-mechanical treatment of steels. The atmosphere is inert, so the steel surface will emerge shiny and no subsequent pickling is required. These processes are called Bright Annealing. Nevertheless, sometimes some undesirable and unexpected oxidation of the steel has been reported. This is due to traces of oxygen in the inert gas that normally should be insufficient to cause appreciable oxidation. The gas can contain very low amounts of oxygen, for example 1 ppm (1 volume part per million), but it is still sufficient to promote marked oxidation of the steel, which can sometimes be more than that in air, at the same temperature, as shown by Sabioni et al. [2]. Industrial applications of this work are the coil annealing of steels in presence of refractory which is the source of oxygen in the steel annealing, and in automotive mufflers (hot end).

The growth kinetics and composition of the oxide films formed on the AISI 409 steel surface in the temperature range from 850 °C

* Corresponding author at: Universidade Estadual do Maranhão – CESC/UEMA, Brazil.
E-mail addresses: fatima.salgado@pq.cnpq.br (M. de Fátima Salgado), vlins@deq.ufmg.br (V.F.C. Lins).

https://doi.org/10.1016/j.engfailanal.2019.07.011
Received 25 November 2018; Received in revised form 23 May 2019; Accepted 1 July 2019
Available online 03 July 2019
1350-6307/

to 950 °C in synthetic air containing 20 wt% of O_2 was recently studied [3]. Chemical analysis indicated that chromium is the main element in the oxide film formed at 850 °C. Other alloying elements such as silicon and titanium are found in small amounts in the oxide film formed up to 900 °C. The oxidation rate increased as the temperature increased.

Salgado et al. [4] studied the high temperature oxidation behavior of AISI 430A and AISI 430E ferritic stainless steels (FSS) at low oxygen pressures and high temperatures. The AISI 430A steel is ferritic up to 860 °C. Above this temperature, this steel is biphasic with austenite and ferrite. The 430E steel is stabilized with niobium and is ferritic at all temperatures. The oxidation behaviors of AISI 430A and AISI 430E SS were different. At 850 °C, the oxidation rate of the 430A steel is higher than the rate of 430E steel, but above 900 °C the oxidation rate of the 430A steel is lower than that of the 430E steel.

The phenomenon of chromium vaporization from chromium alloys exposed to high temperatures is well known. The extent of chromium vaporization of AISI 441, AISI 430 and Mn−Co spinel coated AISI 441 and AISI 430 coated was measured in an atmosphere of 5% H_2O in O_2 over the temperature range 650–900 °C [5]. Among the uncoated steels, the AISI 441 FSS showed a lower chromium vaporization rate compared with the AISI 430. The Mn−Co spinel coating reduced chromium vaporization rate from the AISI 430 surface. However, in contrast, the Mn−Co spinel coating on AISI 441 not only failed to suppress chromium vaporization but increased it.

Nodule formation during the initial stages of oxidation of the AISI 441 at 800 °C in a 5% H_2O in O_2 atmosphere was studied [6]. The oxide scale consisted of a $(Mn,Cr)_3O_4$ spinel top layer and a Cr_2O_3 rich sub-layer alongside oxide nodules growing in places. These nodules with sizes in the micrometer range were studied by using FIB tomography. This study revealed a complex structure and that nodule development is strongly linked to the presence of niobium and/or titanium compound(s) in the substrate.

This study reports the effect of traces of oxygen in the inert gas on the oxidation behavior of AISI 441 FSS. The AISI 441 is a ferritic stainless steel at all temperatures [4]. Previous studies about steel oxidation at high temperatures in the range 850–950 °C and at low oxygen pressures have been considered for comparison [2–4,7–9]. The parabolic oxidation kinetics of the AISI 441 steel and the presence of Cr as a major metallic component indicate that the growth rate of the protective chromia layer formed on the steel surface should be controlled by cation and/or oxygen ion diffusion through the scale layer [10].

2. Materials and methods

The AISI 441 FSS was supplied by APERAM South America. The chemical composition of the steel, shown in Table 1, was provided by the manufacturer.

Samples 10 × 10 × 0.6 mm were cut and ground with 1100, 1200 and 2000 grade SiC paper, and then polished with 3 and 1 μm diamond paste. The oxidation studies were performed in a tubular furnace at 850 °C, 900 °C and 950 °C, in a dynamic atmosphere of synthetic air, for 2, 4, 8, 16, 32 and 50 h to grow a chromia layer on the polished surface of the steel and in a SETARAM TGDTA 92 thermo-balance, with sensitivity of ± 1 μm in the range from 850 °C to 950 °C during 50 h in a dynamic atmosphere of argon with 1 ppm of oxygen, maintained under total pressure of 1 atm. The partial pressure of oxygen in Ar + 1 ppm O_2 was considered to be equal to 10^{-6} atm and in air, 0.21 atm.

The oxidation kinetic was established by measuring the mass gain per unit area (DM/S), where DM is the mass variation, and S is the area of the sample, as a function of oxidation time (t). The microstructures of the oxide films were examined by using the scanning electron microscopy (SEM), and the chemical composition was determined by the energy dispersive X-ray spectroscopy (EDS). Phase analysis was performed by using the Grazing X-ray diffraction (XRD) with 8 KeV energy.

3. Results

3.1. Oxidation kinetics

The values of mass gain per unit area (ΔM/S) as a function of oxidation time (t) were obtained. The maximum error associated with the mass gain measurements was 10%. The average mass gain error was 7%. The curves of mass gain as a function of duration of oxidation carried out in a tubular oven at 850 °C, 900 °C and 950 °C in synthetic air are shown in Figs. 1 and 2. Figs. 3 and 4 show the oxidation behavior of the steel at 850 °C, 900 °C and 950 °C, in argon atmosphere with 1 ppm of oxygen for 50 h, as determined in a thermal balance. Comparison of the oxidation behavior in air and in argon atmosphere is shown in Fig. 5.

Oxidation follows parabolic kinetics, indicating that oxidation was controlled by cation diffusion and/or by oxygen through the oxide film [10]. According to the Wagner theory of oxidation, oxide layers grow from the metal substrate outward and from the outer oxide film inward. The metal cations and electrons, which are produced at the metal/oxide interface, diffuse outward through the oxide layer. Oxygen is reduced to O^{2-} anions at the atmosphere/oxide interface and the anions diffuse towards the oxide/metal interface [11].

In air, the oxidation rate of the AISI 441 FSS increased as the temperature increased (Fig. 1). In argon with 1 ppm of oxygen, the

Table 1
Chemical composition of the AISI 441 FSS (wt%).

Steel	C	Mn	Si	P	Nb	S	Cr	Ni	Ti
441	0.03	1.00	1.00	0.04	0.3–1.00	0.015	17.5–18.5	0.50	0.10–0.60

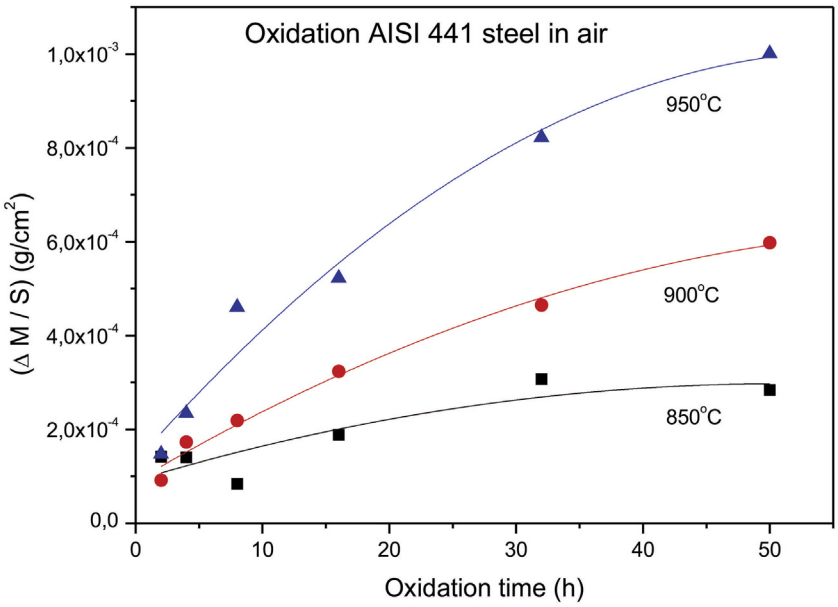

Fig. 1. Mass gain of AISI 441 at 850 °C, 900 °C and 950 °C in synthetic air.

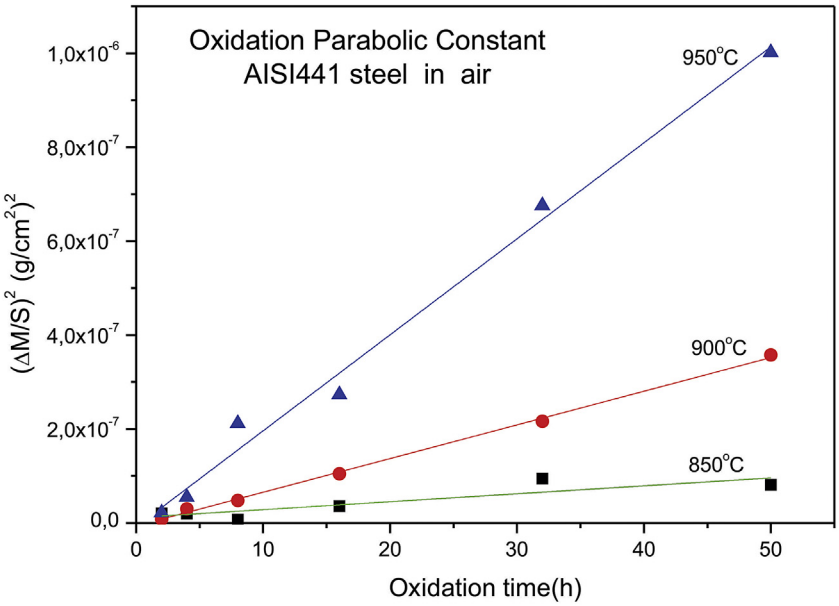

Fig. 2. Parabolic constant of AISI 441 at 850 °C, 900 °C and 950 °C in synthetic air.

oxidation rate decreased as the temperature increased (Fig. 3). The oxidation rate of the AISI 441 FSS is higher in argon with 1 ppm of oxygen than in synthetic air (Fig. 5).

The parabolic kinetics during oxidation are described by the ratio: $(DM/S)^2 = kpt + ko$, where "kp" is the parabolic oxidation rate constant and "ko" is a constant. The "kp" constant was established from graphs of $(\Delta M/S)^2$ as a function of time (Figs. 2 and 4).

When oxidation kinetics follow a parabolic law, the graph of $(\Delta M/S)^2$ as a function of the oxidation time (t) is a straight line, wherein the angular coefficient is the parabolic rate constant, "kp". The parabolic constant values are shown in Table 2.

3.2. Microstructure of the oxide films

Fig. 6 shows a random distribution of oxides on the surface of the AISI 441 FSS. Oxide nodules nucleated with a specific orientation following the risks of polishing on the surface of oxidized steel at 900 °C as shown in Fig. 7. Fig. 8 shows more oxide nodules in the volume of the grains and at the grain boundaries on the surface of AISI 441 FSS oxidized at 950 °C. The oxide nodules were

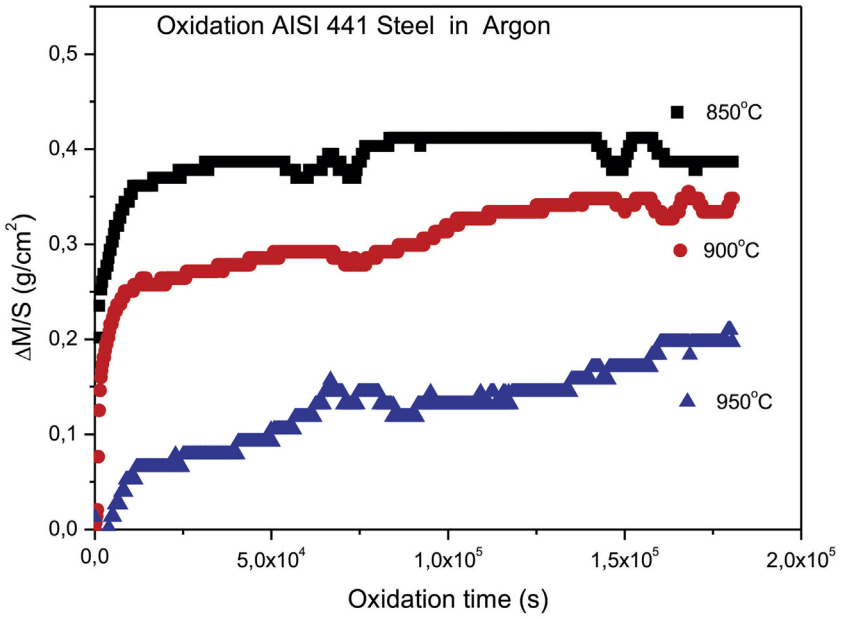

Fig. 3. Mass gain of AISI 441 at 850 °C, 900 °C and 950 °C in argon atmosphere with 1 ppm of oxygen.

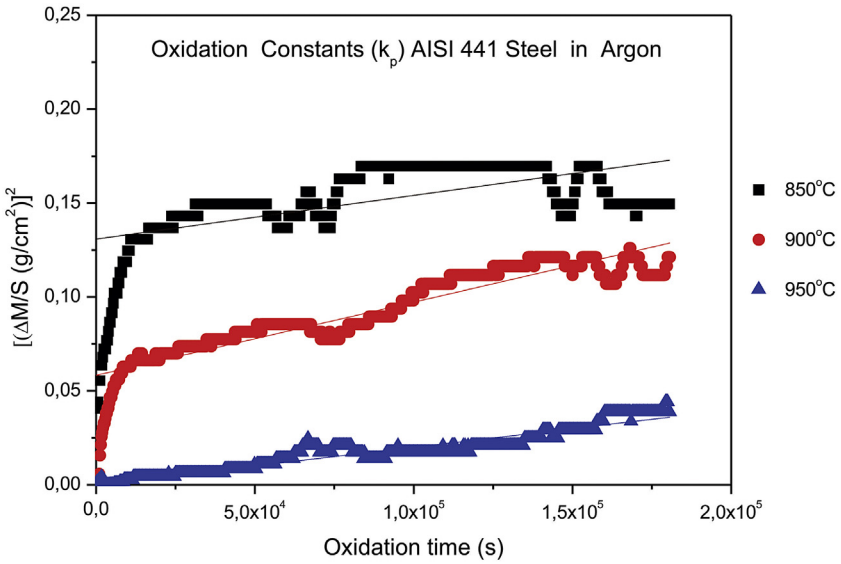

Fig. 4. Parabolic constant of AISI 441 at 850 °C, 900 °C and 950 °C in argon atmosphere with 1 ppm of oxygen.

indicated in Figs. 6 to 8 by arrows.

The samples oxidized in argon with 1 ppm of oxygen showed prismatic shaped oxides on their surfaces and their crystal size decreased as the temperature increased as shown in Figs. 9, 10 and 11.

3.3. Chemical composition of oxide films

3.3.1. EDS results of oxide films

Fig. 12 shows the oxidized surface of the AISI 441 FSS at 850 °C in argon with 1 ppm of oxygen atmosphere. The EDS spectra shown in Figs. 13 and 14 correspond to the points 1 and 2 in Fig. 12. The results obtained at 850 °C are similar to the results observed on samples oxidized at 900 °C and 950 °C. EDS analysis shows chromium as the main metallic element in the oxide films formed under all experimental conditions. Lower contents of Mn, Ti, Fe and Si were also identified in the oxide films.

Fig. 15 shows the scanning electron micrograph of the surface of the AISI 441 sample oxidized at 950 °C in synthetic air. The EDS results indicate chromium as the main metallic element in the oxide layer in one region (named as 7 and 8 in Fig. 15) and in another

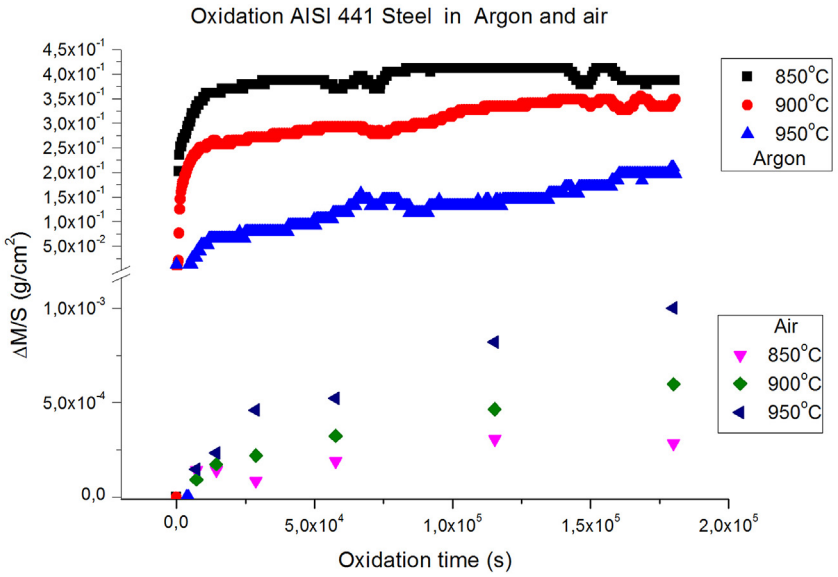

Fig. 5. Mass gain of AISI 441 in argon with 1 ppm of oxygen and in synthetic air.

Table 2
Parabolic constants, "kp" (g^2/cm^4s), after isothermal oxidation of the AISI 441 FSS for 50 h in synthetic air and argon with 1 ppm of oxygen.

"kp" ($g^2 \cdot cm^{-4} \cdot s^{-1}$) – AISI 441 Stainless steel		
Temperature (°C)	Synthetic air	Argon + 1 ppm O_2
850	9.7×10^{-13}	1.6×10^{-9}
900	1.7×10^{-12}	8.9×10^{-10}
950	6.0×10^{-12}	7.4×10^{-11}

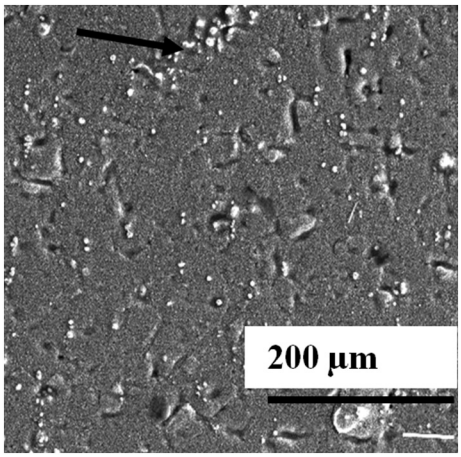

Fig. 6. Scanning electron micrograph of AISI 441 oxidized at 850 °C in synthetic air.

region where spalling of oxide probably occurred (object 5 and 6 in Fig. 15), iron as the main metallic element. Mn, Ti, Si were also identified in the oxide layer.

3.3.2. XRD results of the oxide film

The spectra obtained by Grazing Angle X-ray Diffraction (GAXRD) are shown in Figs. 16, 17 and 18 showing the oxides formed on the steel surface in argon with 1 ppm of oxygen. The main oxide found on the 441 SS surface oxidized at 850 °C was the $MnCr_2O_4$ spinel, and the main oxide identified on the surface of the AISI 441 SS oxidized at 900 °C was a titanium, chromium and niobium

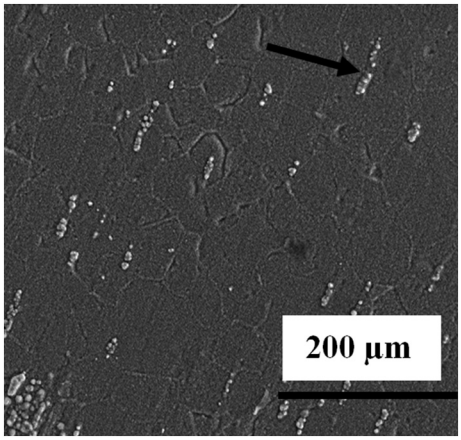

Fig. 7. Scanning electron micrograph of AISI 441 oxidized at 900 °C in synthetic air.

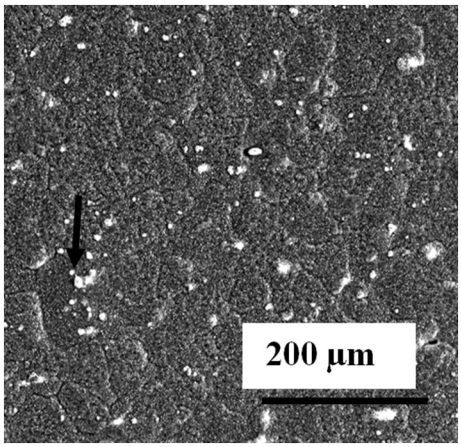

Fig. 8. Scanning electron micrograph of AISI 441 oxidized at 950 °C in synthetic air.

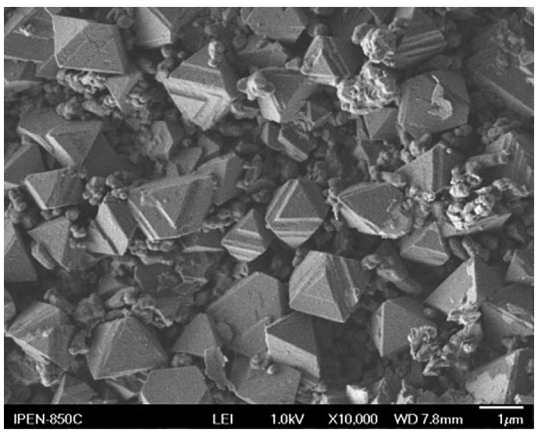

Fig. 9. FEG micrograph of surface of the AISI 441 oxidized at 850 °C in argon with 1 ppm of oxygen.

oxide, $Ti_4Cr_2Nb_2O_4$. The Cr_2O_3 was identified as the main oxide formed after oxidation of AISI 441 SS at 950 °C.

The oxides formed after oxidation of the AISI 441 FSS in an atmosphere of argon with 1 ppm oxygen at 850 °C were $MnCr_2O_4$, Cr_2O_3 and $Cr_2P_6O_{18}$. At 900 °C, the $Ti_4Cr_2Nb_2O_4$, Cr_2O_3, Mn_2SiO_4, SiO_2, and Cr_3Nb_3C phases were identified. At 950 °C, the compounds found on the surface of the AISI 441 FSS oxidized in argon with 1 ppm of oxygen were Cr_2O_3, Mn_2SiO_4, SiO_2, Cr_3Nb_3C, Cr_3C_2. In an atmosphere of argon with 1 ppm of oxygen, the lowest mass gain was obtained for the sample oxidized at 950 °C and at this

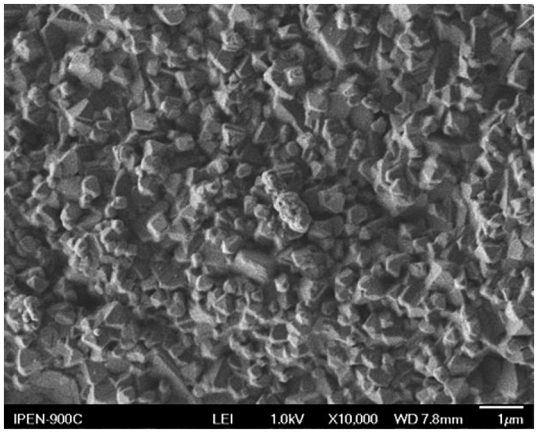

Fig. 10. FEG micrograph of surface of the AISI 441 FSS oxidized at 900 °C in argon with 1 ppm of oxygen.

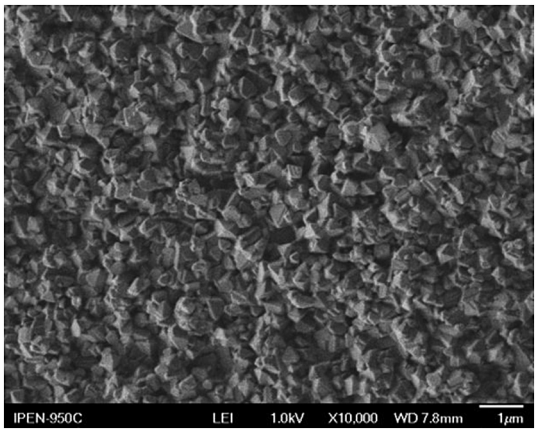

Fig. 11. FEG micrograph of surface of the AISI 441 FSS oxidized at 950 °C in argon with 1 ppm of oxygen.

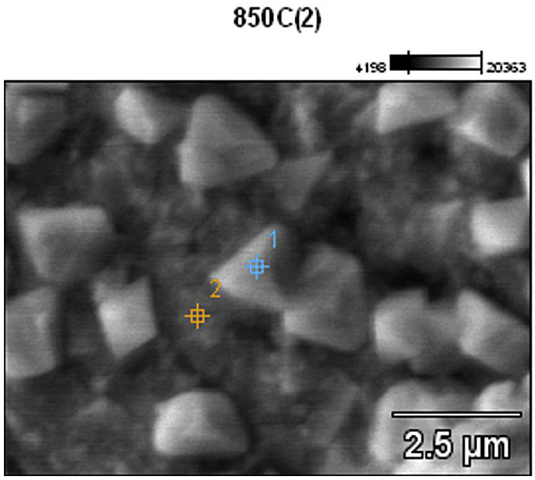

Fig. 12. Oxidized surface of the AISI 441 steel at 850 °C in argon with 1 ppm of oxygen.

temperature, the main oxide identified by using GAXRD was the protective oxide of Cr_2O_3.

Analysis by Grazing Angle X-ray Diffraction (GAXRD) showed that phases in oxide films formed in synthetic air, in the temperature range from 850 °C to 950 °C, are spinels of chromium, manganese and iron with chromium oxide being the main constituent. In argon atmosphere with low oxygen content, the main phases that were identified in the oxide layer on the surface of the AISI 441

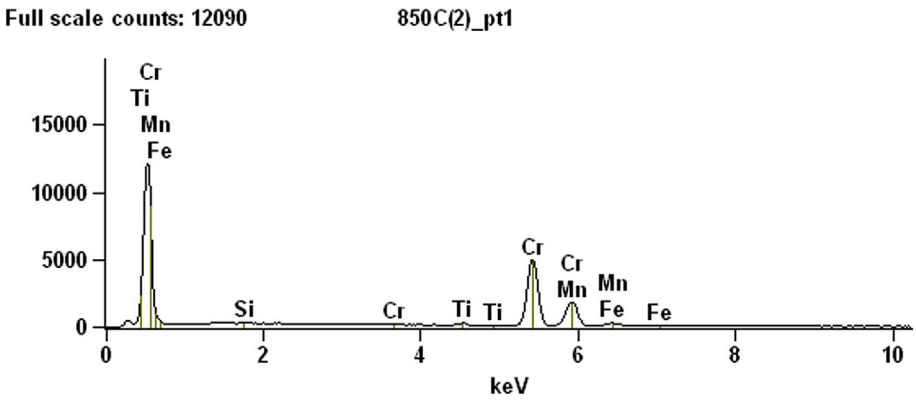

Fig. 13. EDS spectrum of point 1 on the surface of the 441 FSS at 850 °C in argon with 1 ppm of oxygen.

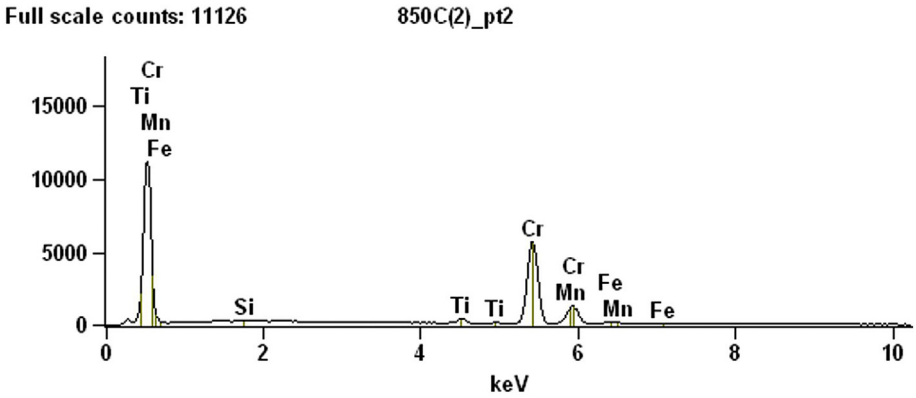

Fig. 14. EDS spectrum of point 2 on the surface of the 441 FSS at 850 °C in argon with 1 ppm of oxygen.

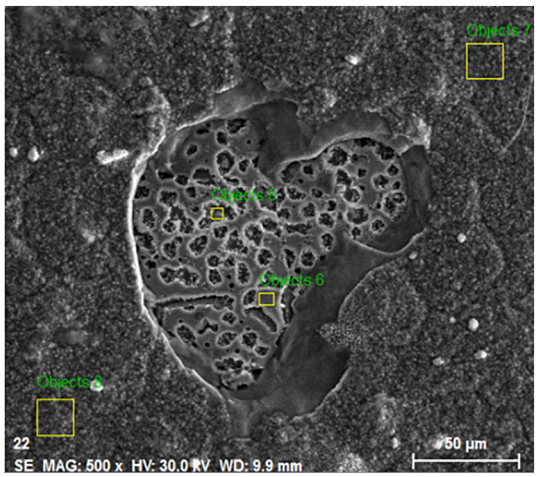

Fig. 15. SEM micrograph of the surface of the AISI 441 FSS at 950 °C in synthetic air showing chromium rich regions (7 and 8) and iron rich regions (5 and 6 inside a central crater).

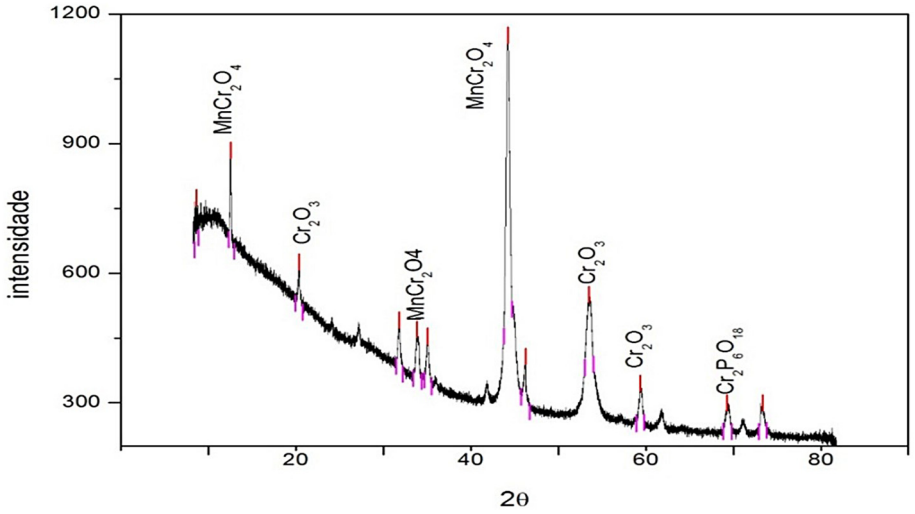

Fig. 16. Diffractogram of surface of AISI 441 oxidized at 850 °C in argon with 1 ppm of oxygen.

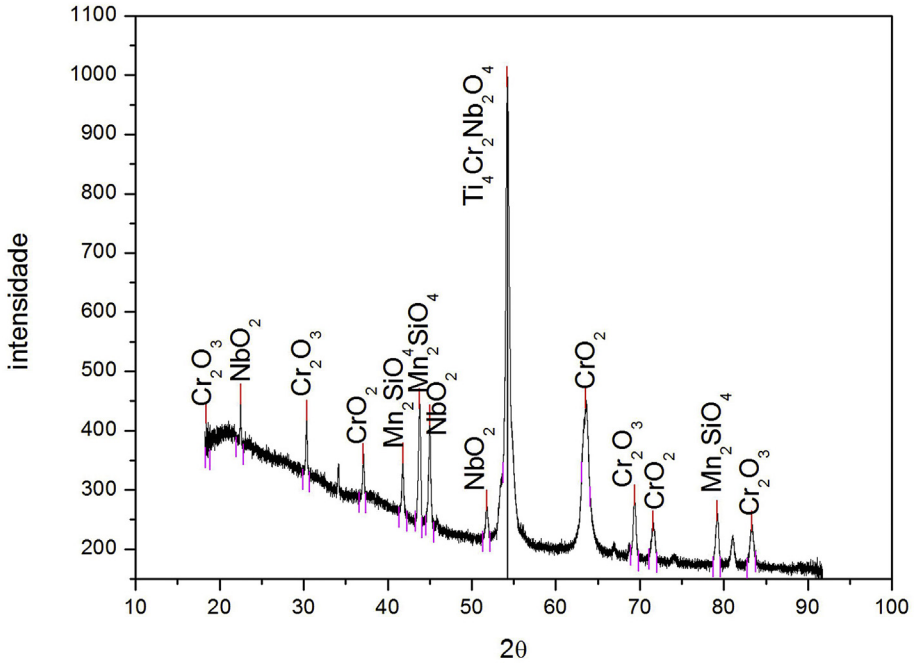

Fig. 17. Diffractogram of surface of AISI 441 oxidized at 900 °C in argon with 1 ppm of oxygen.

FSS are $MnCr_2O_4$ spinel in sample oxidized at 850 °C, $Ti_4Cr_2Nb_2O_4$ and Mn_2SiO_4 in sample oxidized at 900 °C and Cr_2O_3 in sample oxidized at 950 °C.

4. Discussion

4.1. Comparison of oxidation kinetics of AISI 441 steel

The oxidation behavior of AISI 441 FSS in synthetic air and in argon +1 ppm O_2, in the range from 850 °C to 950 °C is shown in Figs. 1 to 5. Figs. 1, 2 and 3 correspond to oxidation in synthetic air wherein AISI 441 FSS exhibited a gradual increase in mass gain as the temperature increased. This was in the range of parabolic oxidation, similar to that determined at the same temperature for oxide growth [2,3]. In synthetic air, the mass gain per unit area increased as the temperature increased as shown in Fig. 1. The oxidation rate increases with temperature according to the Arrhenius equation [11]. The main oxide formed is the chromium oxide, a p-type semiconductor, which increases the oxidation rate as the temperature increases. The chromium oxide is a protective oxide which

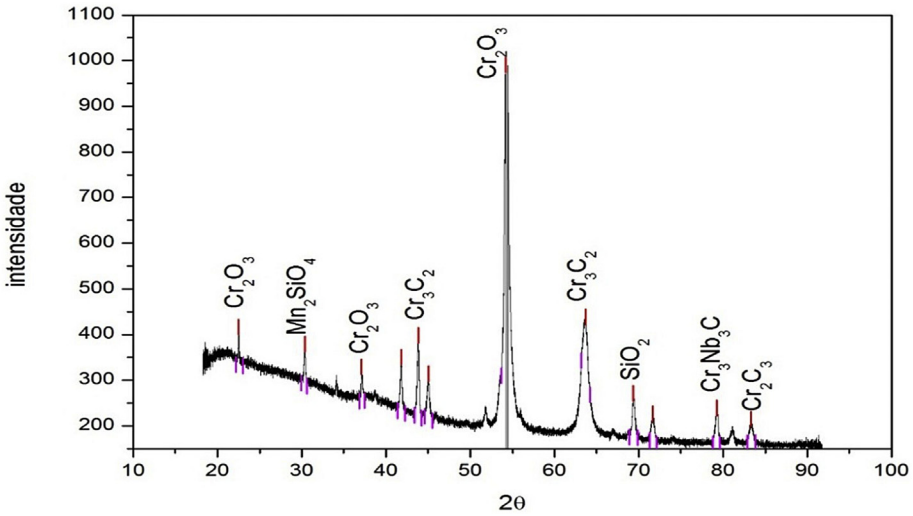

Fig. 18. Diffractogram of surface of AISI 441 oxidized at 950 °C in argon with 1 ppm of oxygen.

presents a Pilling-Bedworth ratio of 2.07, indicating the formation of a compact, uniform layer covering the metal surface. However, the Pilling-Bedworth ratio is only one factor in determining the oxidation resistance of metals at high temperatures. The properties required for the oxide to be protective are a low vapor pressure, a high melting point, a good adherence to the substrate, good high-temperature plasticity, low electrical conductivity, a coefficient of expansion approximately equal to that of the metal, and a Pilling-Bedworth ratio of approximately one.

In the atmosphere of argon with 1 ppm of oxygen, in the temperature range from 850 °C to 950 °C, the oxidation kinetics exhibited two different rates of mass gain. Initially, a higher mass gain rate and then the oxidation rate decreased to being constant over time. The second oxidation rate decreased as the temperature decreased. However, for the lowest temperature, although the oxidation progressed less over time, the mass gain per area was the highest. The oxides formed at 850 °C and 900 °C were mainly those of manganese, titanium and niobium, all n-type semiconductors. It is well known that for n-type semiconductors, the mass gain per area increases as the oxygen pressure decreases [11]. The dependence of the parabolic rate constant with oxygen pressure is $P(O_2)^{-1/6}$ or $P(O_2)^{-1/4}$ if the semiconductor is n-type with interstitial cations or anion vacancies [11]. The main oxide formed at 950 °C in the atmosphere of argon with 1 ppm of oxygen is chromium dioxide which is a p-type semiconductor with cation vacancies. In this case, the dependence of parabolic rate constant with oxygen pressure is $P(O_2)^{1/6}$ or $P(O_2)^{1/4}$ [11]. At lower oxygen pressures, the parabolic constant and the oxidation rate are lower for chromia at 950 °C. Thus, as shown in Fig. 5, in argon with 1 ppm of O_2, the mass gain per unit area at 850 °C and 900 °C are higher than the mass gain per unit area at 950 °C, after 50 h of oxidation. This behavior was observed previously during oxidation of AISI 430A steel in Ar-H_2-H_2O atmosphere with a low oxygen partial pressure [4]. However, at 950 °C the mass gain continued to increase after 50 h of oxidation while, at the lowest temperature, the mass gain remained almost constant after the initial mass gain. The rate of mass gain increased with increasing temperature. At 900 °C, a clear tendency for nucleation of oxides was observed and these followed a specific orientation, mainly at polishing risks, as already reported in the literature [12].

An explanation for the lower mass gain of AISI 441 steel in synthetic air would be volatilization of chromium oxide although the volatilization occurs mainly near 1000 °C. Appreciable volatilization occurred in oxygen, but none in argon. Fe_2O_3 showed volatilization in none of these atmospheres [13]. The evaporation occurs by oxidation of Cr_2O_3 to gaseous CrO_3 which dissociates to Cr_2O_3 on redeposition [13]. Volatile Cr species are formed on the steel surface when oxygen and water vapor react with the Cr-rich surface oxide. One volatile specie formed is $CrO_2(OH)_2$ [14]. However, in argon atmosphere with low oxygen content this reaction is suppressed, the chromium oxide is not volatilized, and the mass gain is higher in argon with 1 ppm of oxygen than in air.

Figs. 3 to 5 show that oxidation caused by trace amounts of oxygen in the argon atmosphere does not work as a protective gas against oxidation. On the basis of these results, it can be observed that argon gas with trace amounts of oxygen, as used in this study, and under experimental conditions, also used in this study, does not function as a protective gas against oxidation.

4.2. Morphology and chemical composition of the oxide films

In synthetic air at 850 °C, the oxide films formed are dispersed grains. There is no significant difference in composition of the equiaxial grains. The round shaped grains contain mainly Cr, Ti and Mn, corresponding to a spinel of $MnCr_2O_4$ and TiO_2. This observation is in good agreement with [4–6]. EDS results showed that in the oxide film formed on the AISI 441 surface, the higher the temperature the higher the Cr content. The Mn content in the oxide scale increased as the temperature increased. On the other hand, the particle size increased progressively as the temperature increased, indicating that the detected $(Mn,Cr)_3O_4$ spinel was the top layer [6]. At some of the points that were analyzed, only Cr and Mn were detected (Figs. 13–15), and this suggests the formation of

$MnCr_2O_4$ spinel particles on the outer surface. The presence of Mn on chromia forming alloys has been discussed by Sabioni et al. [15]. The presence of Mn as a solute in the chromium oxide causes the decrease in oxidation rate according to the Hauffe rules [11]. On the basis of their study of Mn diffusion in chromia films, Sabioni et al. [15] suggested that Mn-rich particles on the outer surface result from the initial oxidation, due to the higher affinity of manganese for oxygen than that of chromium. This is followed, in a second stage, by manganese ion diffusion through chromia towards the outer surface of the scale. The amount of Mn in the surface of the film is limited due to the low Mn content in the steel, compared to chromium. Chromium is the main metallic element in oxide films, and Mn, Ti, and Fe oxides were also found. These four metallic elements are the constituents in the phases detected on oxide films, as shown in item 3.3.2. According to the Hauffe rules of oxidation [11], the presence of a titanium as a solute in chromia increases the defect concentration, the ionic diffusion, and the oxidation rate. Considering that chromium oxide does not act as a barrier for diffusion of manganese and iron, ions of Mn and Fe from their oxides formed at the beginning of oxidation can be found spread throughout the chromium oxide film, favoring the formation of phases containing manganese or iron, as observed by X-ray diffraction.

In argon atmosphere with 1 ppm of oxygen, the main phases identified in the oxide layer on the surface of the AISI 441 oxidized at 850 °C were $MnCr_2O_4$ spinel, $Ti_4Cr_2Nb_2O_4$ and Mn_2SiO_4 on samples oxidized at 900 °C and Cr_2O_3 on the surface of samples oxidized at 950 °C. The presence of n-type semiconductors such as Mn, Ti, Nb oxides which contribute to a higher parabolic constant as the oxygen pressure decreased, should explain the higher oxidation rate of AISI 441 in argon with a low oxygen content than in synthetic air. Chromium and niobium carbides were also detected on the surface of AISI 441 oxidized at 950 °C. The presence of these carbides could be contributing to increasing mass gain that was observed at 950 °C at the end of oxidation.

The presence of significant amounts of n-type semiconductors such as titanium, manganese, niobium oxides besides Fe_2O_3, contributes towards the high mass gain at low oxygen partial pressure at the lower temperatures. McCafferty [11] reported that the parabolic rate constant increased as the partial pressure of oxygen decreased for n-type semiconductors. On AISI 441 oxidized at 950 °C in argon with 1 ppm of oxygen (Fig. 18), the main phase identified by XRD was chromia, which is a p-type semiconductor. In this case, the parabolic rate constant increased as the oxygen partial pressure increased. Thus, the mass gain of the AISI 441 in argon with 1 ppm oxygen was lower at 950 °C than that at 900 °C and this, even lower than that at 850 °C.

5. Conclusions

A comparative study of the oxidation behavior of ferritic stainless steel AISI 441 in argon containing 1 ppm of oxygen and in synthetic air was carried out in the temperature range from 850 °C to 950 °C for 50 h.

Under all the experimental conditions, the oxide film growth on the AISI 441 followed a parabolic law.

The oxidation resistance of the AISI 441 FSS was higher in synthetic air than in argon with 1 ppm of oxygen, in the temperature range from 850 °C to 950 °C. In synthetic air, after 50 h of oxidation, the mass gain per unit area of AISI 441 increased as the temperature increased. In argon with 1 ppm of oxygen, the mass gain per unit area of AISI 441 after 50 h of oxidation increased as the temperature decreased. In argon with 1 ppm of oxygen, in the initial stages, a higher mass gain rate was observed and then the oxidation rate decreased and remained constant over time. The second oxidation rate decreased as the temperature decreased.

X-ray diffraction analysis of the oxide formed in argon atmosphere with 1 ppm of oxygen confirmed that: (a) Cr_2O_3 is the main phase in the oxide film formed at 950 °C; (b) the presence of mainly $MnCr_2O_4$ spinel in the oxide film formed at 850 °C; (c) the main presence of $Ti_4Cr_2Nb_2O_4$ and Mn_2SiO_4 in the oxide film formed at 900 °C. In the oxide formed on the AISI 441 surface at 950 °C in argon with 1 ppm of oxygen, chromium and niobium carbides were identified. The stabilizing elements such as Nb, Mn and Si, present in very small amounts in the stainless steel, formed complex oxides. Analysis by Grazing Angle X-ray Diffraction (GAXRD) showed that phases in oxide films formed in synthetic air, at 850 °C to 950 °C, were spinels of chromium, manganese and iron with chromium oxide as the main phase. The Cr_2O_3 content in the oxide layer on oxidized AISI 441 FSS increased as the temperature increased in atmospheres of argon with 1 ppm of oxygen and in synthetic air.

Acknowledgments

The authors are grateful to CNPq, FAPEMA and Centro de Microscopia of UFMG for the studies carried out in synthetic air, to IPEN for studies done in argon and to the Laboratório Nacional de Luz Sincroton (Brazil) for X-ray diffraction analysis. The authors are grateful to Thais Mendes and Jack for English revision and to Cassio Rêgo for technical support.

Declaration of Competing Interest

We declare that there is no conflict of interest.

References

[1] M.F. Salgado, S.C.S. Rodrigues, D.M. Santos, A.S. Brandim, V.F.C. Lins, Cyclic oxidation resistance of ferritic stainless steels used in mufflers of automobiles, Eng. Fail. Anal. 79 (2017) 89–97.

[2] A.C.S. Sabioni, A.M. Huntzb, M.F. Salgado, A. Pardini, E.H. Rossi, R.M. Paniago, V. Ji, Atmosphere dependence of oxidation kinetics of unstabilized and Nb-stabilized AISI 430 ferritic stainless steels in the temperature range 850–950°C, Mater. High Temp. 27 (2) (2010) 89–96.

[3] E.C. Serra, A.S. Brandim, G.B. Oliveira, M.F. Salgado, High temperature oxidation of ferritic stainless steel AISI 409 in atmosphere synthetic air, Rev. Bras. Apl. Vac. 34 (1) (2015) 14–23.

[4] M.F. Salgado, A.C.S. Sabioni, A.M. Huntz, E.H. Rossi, High temperature oxidation behaviour of the AISI 430A and AISI 430E stainless steels in Ar/H2/H2O atmosphere, Mater. Res. 11 (2008) 227–232.
[5] W. Wongpromrat, H. Thaikan, W. Chandra – ambhorn, S. Chandra- ambhorn, Chromium vaporisation from AISI 441 stainless steel oxidised in humidified oxygen, Oxid. Met. 79 (2013) 529–540.
[6] W. Wongpromrat, V. Parry, F. Charlot, A. Crisci, L. Latu-Romain, W. Chandra-ambhorn, S. Chandra-ambhorn, A. Galerie, Y. Wouters, Possible connection between nodule development and presence of niobium and/or titanium during short time thermal oxidation of AISI 441 stainless steel in wet atmosphere, Mater. High Temp. 32 (2015), https://doi.org/10.1179/0960340914Z.00000000057.
[7] A.M. Huntz, A. Reckmann, C. Haut, C. Sévérac, M. Herbst, F.C.T. Resende, A.C.S. Sabioni, Oxidation of AISI 304 and AISI 439 stainless steels, Mater. Sci. Eng. A 447 (2007) 266–276.
[8] A.C.S. Sabioni, A.M. Huntz, E.C. Luz, M. Mantel, C. Haut, Comparative study of high temperature oxidation behaviour in AISI 304 and AISI 439 stainless steels, Mater. Res. 6 (2003) 179–185.
[9] M.F. Salgado, A.C.S. Sabioni, Estudo do efeito da pressão de oxigênio sobre a oxidação dos aços inoxidáveis ferríticos AISI 430A, AISI 430E e AISI 444 em altas temperaturas, Tese de doutorado, REDEMAT, Universidade Federal de Ouro Preto, Ouro Preto, 2009.
[10] C. Wagner, Diffusion and High Temperature Oxidation of Metals. Atom Movements, ASM, Cleveland, 1951.
[11] E. McCafferty, Introduction to Materials Science, Springer, New York, 2010.
[12] V.F.C. Lins, E.M.P. Silva, Características estruturais e cinéticas da oxidação ao ar de liga Fe-Mn-Al-C, Met. Mater. 44 (1988) 1265–1268.
[13] D. Caplan, M. Cohen, The volatilization of chromium oxide, J. Electrochem. Soc. 108 (1961) 438–442.
[14] E.J. Opila, D.L. Myers, N.S. Jacobson, I.M.B. Nielsen, D.F. Johnson, J.K. Olminsky, M.D. Allendorf, Theoretical and experimental investigation of the thermochemistry of $CrO_2(OH)_2(g)$, J. Phys. Chem. A 111 (2007) 1971–1980.
[15] A.C.S. Sabioni, A.M. Huntz, L.C. Borges, F. Jomard, First study of manganese diffusion in Cr_2O_3 polycrystal and thin films, Philos. Mag. A 87 (2007) 1921–1937.